

AIRWATCH: the Fast Detector

Anna Gregorio^a, Roberto Stalio^{a,b}, Ezio Alippi^c, Giovanni Bonanno^d, Luciano Bosisio^e, Pietro Bruno^d, Rosario Cosentino^d, Rosario Di Benedetto^d, Flavio Fontanelli^f, Gianrossano Giannini^e, Valerio Gracco^f, Anna Lenti^c, Alessandro Petrolini^f, Mario Sannino^f, Livio Scarsi^g, Salvatore Scuderi^d, Paolo Trampus^a, Andrea Vacchi^h

^a Center for Advanced Research in Space Optics, Area Science Park, Trieste

^b Dipartimento di Astronomia, Università di Trieste

^c Laben S.p.A., Milano

^d Osservatorio Astrofisico di Catania

^e Dipartimento di Fisica, Università di Trieste

^f Dipartimento di Fisica, Università di Genova & INFN, Sezione di Genova

^g Istituto di Fisica Cosmica e Informatica - CNR, Palermo

^h INFN, Sezione di Trieste

ABSTRACT

The discovery of the Extreme Energy Cosmic Rays (EECR) with energy greater than 10^{20} eV has opened a new research branch of astrophysics on both observational and interpretative point of views. Together with the EECR one has also to consider the neutrino component which, independently on its primary or secondary origin, can reach comparable energies. These particles can be detected through the giant showers (EAS) produced in the Earth atmosphere and the induced fluorescent molecular nitrogen emission. Observing the EECR "signals" is very difficult; we need forefront technology or new developments. The main reason is that their flux is very weak, typically of the order of a few events/year/1000 km² per EECR of $E \approx 10^{20}$ eV. The proposed AirWatch mission, based on a single orbiting telescope which can measure both intensity and direction of the EAS, impose new concepts for the detectors: single photon sensitivity, fast response of the order of few microseconds with sampling times of tenths of nanoseconds, low noise and good S/N ratio, large area (linear dimension of the order of several tenths of cm), adaptability to a curved surface. Fortunately the spatial resolution requirements are somehow relaxed. The peculiar characteristics of this application are such that no available detectors satisfies completely the requirements. Therefore the final detector has to be the result of a R&D program dedicated to the specific problem. In this paper we survey a number of possible detectors and identify their characteristics versus the AirWatch mission requirements.

Key words: AirWatch mission, Extreme Energy Cosmic Rays (EECR), Earth Atmospheric Showers (EAS), segmented-type detectors, projective detectors

1. INTRODUCTION

The discovery of cosmic rays with energy larger than 10^{20} eV¹ (Extreme Energy Cosmic Rays - "EECR") opened a new chapter in Astrophysics, both from observational and theoretical points of view. Their origin, currently one of the most interesting and controversial problems of High Energy Astrophysics², seems directly connected to extremely efficient accelerating mechanisms which are still unidentified. These cosmic rays can be observed by means of the giant showers produced by their interaction with Earth atmosphere. About twenty events with energy larger than 10^{20} eV have been observed so far. This high energy is above the maximum allowed by the interaction with the cosmic background

radiation over cosmological distances (GZK effect).

The observational technique which has been chosen as the most promising consists in the detection of nitrogen fluorescence light produced by these extended air showers (EAS). This emission, directly related to the number of particles in the shower, allows to determine the EAS evolution in the atmosphere, to measure its energy and to determine the direction of the primary cosmic ray. In this approach the atmosphere is at the same time absorber and signal generator. The observation of these events shows problems which are at the limit of present technology. In fact, being them neutrinos, photons or charged particles, their flux is extremely low, typically of the order of few events/year/1000 km² for EECR of $E \approx 10^{20}$ eV. Neutrinos have the additional problem of their very feeble interaction with matter.

Some international projects are under study and definition; they use both Earth based telescopes (Auger project³) and space telescopes (OWL⁴ and AirWatch^{5,6} projects). Observations from space guarantee better sensitivity as a larger atmospheric mass can be observed (minimum dimension of the order of a thousand and possibly a million of km²). Therefore a larger number of events is expected. The observation from space might also allow to detect γ -ray bursts and possible showers induced by very high energy neutrinos traveling at low inclination. This fact will make it possible to study correlation between charged particles, photons and neutrinos coming from cosmic objects.

The two space projects under study, OWL and AirWatch, are based on a different concept for shower detection. OWL is basically an interferometer, i.e. it consists of two satellites with imaging telescopes and current technology detectors which provide a stereoscopic view of the scene. EAS intensity and direction are directly obtained. AirWatch is a single telescope which can measure by itself not only the intensity but the direction as well by taking advantage of very fast, new technology, detectors which allow a 3-D reconstruction of the shower⁷. In this paper we discuss several possible options for the AirWatch focal plane detector.

2. DETECTOR REQUIREMENTS

The one-satellite choice for AirWatch requires a detector system of new concept integrated into a large aperture, large field of view, optical system able to observe a very large atmospheric mass (of the order of 10^{13} ton of Earth atmosphere). The detector has the following characteristics:

1. single photon sensitivity in the 330-400 nm wavelength range which includes atmospheric N₂ fluorescent emission bands (the atmosphere is relatively transparent at these wavelengths);
2. fast response (of the order of few microseconds with sampling times of tenths of nanoseconds) to determine the shower direction and avoid the pile-up of photons produced by the EAS;
3. low noise and good S/N ratio to detect the faint signal produced by the less energetic showers ($E \sim 10^{19}$ eV) and discriminate them from the background (for merging the observed energy spectrum with the observations from previous, lower energy, experiments);
4. capability of determining the position of arriving photons as a function of time and follow the space-time development of the shower;
5. large area (linear dimension of the order of several tenths of cm), due to the large field of view of the optics, and must cover the curved focal surface with a sensitive area as large as possible;
6. adaptability to a concave surface to fit the optical design (for this last requirement more than one detector elements in a mosaic design will be used);
7. spatial resolution not necessarily very high, of the order of a few mm on the detector, corresponding to about 1 km² when projected on Earth.

Other major detector requirements are radiation hardness, low power consumption, low weight, high reliability and stability over long periods. Another crucial element is the definition of an efficient trigger system to select the giant showers with high efficiency and good background rejection.

Two detector classes are envisaged⁸: segmented-type detectors i.e. pixel detectors with a projective dimension of the single pixel of the order the above mentioned resolution and projective detectors. In the case of the pixel detector, the large number of elements (of the order of hundreds of thousands) requires a sophisticated read-out electronics capable to handle such a large number of channels. The high speed requirements are also very difficult to satisfy. The read-out system

for the projective detector class is simpler and the constraint of high speed could be less stringent. However they have noise, background and signal ambiguity problems in image reconstruction. The above items are research priorities for the AirWatch detector system.

3. EXPERIMENTAL KEY PARAMETERS

The input parameters given in Table 1 are preliminary estimates while waiting for the final optical design specifications. Two solutions are currently investigated by the optical people: a catadioptric system (known as Schmidt camera) and a single, or double, plastic molded Fresnel lens. The characteristics of the focal plane detector should satisfy these specifications keeping in mind that the problem is still under study and that modifications or new solutions could be implemented in a future.

Table 1: Experimental input parameters

Optic type	Fresnel	Schmidt
Orbit height	400 km	400 km
FoV	± 25 deg	± 20 deg
Area on Earth (circle of diameter):	≈ 400 km	≈ 300 km
Pixel size at Earth	1 km	1 km
No. of pixels (channels)	400x400	300x300
Focal surface diameter	≈ 1.2 m	≈ 0.60 m
Pixel size on focal plane (paraxial approx)	3.2 mm	2.0 mm
Pixel size on focal plane (at the edge of FoV)	6-7 mm	2 mm
Detector Geometrical Acceptance	$> 80\%$	$> 80\%$
Background events (photons/3.3 μ sec/pixel):	0.2	0.06
Signal events* (photons/3.3 μ sec/pixel):	4	1
Aperture	1000 mm	1000 mm
Focal length	1300 mm	1020 mm

* at $E \approx 1 \times 10^{19}$ eV, hitting a single pixel

4. DETECTOR SELECTION

The peculiar characteristics of this application are such that no available detectors satisfies completely the requirements. In particular, commercial detectors are inadequate in the number of channels and fail to cover the large plane focal surface with good geometrical acceptance. Therefore the final detector has to be the result of a R&D program dedicated to the specific application.

Four types of baseline detectors have been identified belonging to the two classes mentioned above:

1. a pixel detector based on the commercial Active Pixel Sensor, (APS);
2. a pixel detector based on the Multi-Anode PhotoMultipliers Tube (MAPMT);
3. a pixel detector derived from High Energy Physics experiments such as Hybrid Photon Detector (HPD);
4. two projective detectors also derived from High Energy Physics experiments, the Silicon Drift detector (SD2000) and the Silicon Intensified Micro-Strip detector (SIMS).

The R&D program will analyze, test and characterize these types of detectors to define the best solution prior to final development. Test will include precursor flights on stratospheric airplanes or balloons or on the Space Shuttle in the framework of the multi-flight UVSTAR program.

It is to be noted that all the detectors under study have a common electro-optics head, based on a photocathode system for photon conversion to electrons, but they adopt different techniques to detect the electrons and read the image. A constraint

which applies to all detectors considered, is that the photocathode must be protected from exposure to strong light, even when not operating, to avoid damage and lifetime reduction. The response to strong thermal variations must also be checked to avoid mechanical stresses and to prevent a possible sublimation of the photocathode at low temperatures.

4.1 Intensified CMOS-APS

This is an intensified silicon detector operating in photon counting regime⁹. The adopted technique is similar to that used in the intensified CCD which is based on a Microchannel Plate (MCP) coupled with a CCD working as a position detector. In figure 1 a schematic drawing of the detector components is shown. The electrons generated in a photocathode are multiplied by means of a MCP, and the emerging electron cloud impinges on a phosphor screen giving a luminous spot. The phosphor screen is optically coupled to a CMOS-APS (Complementary Metal Oxide Semiconductor - Active Pixel Sensors) through an optical fiber (tapered or face plated). The CMOS-APS is very similar to a CCD; in fact both technologies are based on photosensitive pixels which are placed in silicon, and in both devices photons are converted into electron charge. The main difference between the two technologies lies in the read-out scheme: in the CCD the charge signals are shifted sequentially into a single output node while in the CMOS detector they are partially processed locally within each pixel by standard CMOS circuitry. The technique is similar to that used in all modern microprocessors, memory chips and many ASIC (Application Specific Integrated Circuits) components.

A CMOS image detector uses a single 5 V (3.3 V internal) power supply. The detector pixels have, besides a photosensitive part (photodiode), a signal processing part. Simple amplifiers can be easily integrated into the pixels so that the conversion from light into voltage or current occurs in the pixel itself, thus making the detector an Active Pixel Sensor. Many other functions such as A/D conversion, automatic gain control, X-Y read-out of each individual pixel, can be integrated into the detector by using VLSI (Very Large Scale Integration) techniques. Other useful characteristics are on-chip integration of the timing control and possibility to exchange image resolution for frame rate (windowing), good radiation hardness, compactness. Schematic of a three transistors CMOS pixel is shown in figure 2a; figure 2b gives a diagram of a complete matrix. The photodiode bias is obtained through the "rows multiplexer", the output through the "columns multiplexer". Typical pixel read-out rate of a CMOS-APS detector is about 5 MHz limited by the on chip ADC. Future R&D work is aimed at obtaining a pixel read-out time of about 10 ns that is the required time to address the multiplexer. In this way a 512x512 pixels APS is read in 2.6 ms and a sub-area of 100x100 pixels will require only 100 μ s. Studies devoted to optimize the readout electronics in order to maximize the count rate have already started. The idea is to use a customized version of a CMOS-APS without on-chip ADC and to read the charge of each pixel with an appropriate amplifier and a fast ADC to obtain counting rates higher than 10⁶ cts/s/pixel or even faster in the windowing mode.

4.2 Multi-anode PhotoMultiplier Tubes

Commercial Multi-Anode PhotoMultiplier Tubes¹⁰ (MAPMT) with characteristics close to the requirements, in particular concerning the pixel size, the gain (of the order of 3×10^5 for a 800 V applied voltage), the fast response time (of the order of nanoseconds), and the low weight and dimensions are available. The most recent devices show a very low cross-talk, of the order of 2% but fail to meet the required geometrical acceptance which is less than 0.5. Also the small number of channels of these devices (of order of 100) makes it necessary to use a very large number of them packed on the focal curved surface. Gain and operating stability over long periods, space qualification are key issues which must be studied.

Assuming 64-channels devices, one needs from 1400 to 2500 (depending on the optic) of them to fill AirWatch focal plane. With an applied voltage of about 1 kV the power consumption is of the order of 1 W/device and the total power consumption would then be of the order of 1.5 kW. The weight of about 30 g per device would give a total weight of about 50 kg. In order to relax these weight and power consumption factors, we are considering devices with a larger (i.e. twice) pixel size to be used at the edge of the field of view where the Point Spread Function (PSF) of the optics is expected to be worse.

The small geometrical acceptance of the MAPMT could be improved by means of a suitable collector lens system. This lens, to be placed in front of each device, performs the required final demagnification. This additional optical element

will increase absorption losses but would have the clear advantage of removing dead regions. Aberrations are not critical because the required focal plane spatial resolution is of the order of a few millimeters. The system is presently under study and its success is strongly dependent on the availability of a suitable UV-transmitting plastic material with a good enough UV-transmittivity. The possible integration of the collector lens on the tube itself is also being investigated.

4.3 Hybrid Photon Detectors

They¹¹ consist of a vacuum tube inside which the photoelectrons generated on a suitable photocathode are accelerated and possibly focused by an electrostatic field onto a silicon pixel detector where the ionization produced by the photoelectrons is detected (figure 3). The gain of the device is a linear function of the applied voltage above a threshold of the order of the kV. It reaches a value of about 5×10^3 for a 20 kV applied voltage.

Two different kind of HPDs exist with electrostatic acceleration of the photoelectrons. In the proximity focused version the photocathode is mapped onto an equally sized pixel detector. In the electrostatically focused version a demagnifying factor, up to five, is achieved. The image size is compressed and smaller pixels can be used to readout a larger photocathode without affecting the sensitive area. The pixel detector has the readout electronics chip bump-bonded on the back side inside the vacuum tube; this minimizes the capacity of the connections and allows a fast response, low noise and cross-talk.

The main advantages of the HPD are: a stable and linear gain (due to the dissipative instead of the multiplicative process), a very good single photoelectron response, a very low power consumption, good spatial uniformity, low sensitivity to magnetic fields, fast response time (of the order on nanoseconds) and a wide flexibility in the tube design and pixel layout. The last advantage might be very useful to tune the pixel size to the PSF of the optical system which is expected to change as a function of the distance from the optical axis due to the very large field of view required.

Similarly to the MAPMT, the HPD suffer of low geometrical acceptance and low number of pixels per device; the same solution of focalizing lenses as for the MAPMT can be envisaged. The dissipation of the heat produced by the electronics chip inside the tube, the high vacuum required (of the order of 10^{-9} mbar), the reliability of the bump-bonding and the overall operation stability are additional problems to be investigated. The bump-bonding technique should be easily accomplished with the large pixel dimensions required (not smaller than a few hundreds of microns). The very high voltage needed to operate the device requires a careful design of the high voltage system also to avoid interference between close packed tubes. A vary fast, low power, low noise and small dimension charge preamplifier is required to cope with the low device gain.

4.4 Projective Silicon Detectors

SD2000¹² consists of 1) a MCP which produces the charge multiplication and maintains the spatial information and 2) a silicon drift detector as a read-out system.

The silicon drift chamber¹³ (figure 4) is a special device where the basic idea is the so called "sideward depletion": a silicon wafer of large size can be fully depleted by using a series of cathodes and a small size lateral n^+ electrode which acts as a collecting anode for electrons. On the two wafer sides, many p^+ strips (the cathodes), are symmetrically implanted; the potential of these strips, negative with respect to the anode potential, is such to create a homogeneous drift field for electrons, orthogonal to the strip direction. An ionizing event inside the detector creates pairs of electrons and holes; the holes are quickly collected by the cathode strips while the electron cloud drifts towards the chamber border where it is collected by anodes. The first coordinate is given by the position of the anodes which recorded the electron signal (reconstruction of the charge centroid) while the other coordinate is computed by using the time employed by electrons to drift towards the anodes (once the drift velocity is known). The drift velocity is very sensitive to the temperature and the chamber is provided with an auto-calibration system which continuously monitors the drift velocity.

The silicon drift chamber reaches very high spatial resolutions, of the order of a few tens of microns, with a minimum

number of connections, corresponding to the number of anodes on the chamber borders.

The chamber presents two types of problems for AirWatch applications. The first is related to the intrinsic slowness caused by the limits given by the drift velocity which, in addition to temperature, depends on the potential difference between two contiguous strips. An excessive increase of the potential difference could cause break-down or punch-through phenomena in some junctions. Typical drift times are of the order of few microseconds for distances of 1-3 cm but the chamber can distinguish between multiple events with a precision better than 100 ns. This intrinsic slowness seems incompatible with the AirWatch requirements⁷ for deriving the EECR inclination; however, the SD2000 operating mode is conceptually different than the other detectors. In fact, the chamber visualizes the event projection without any ambiguity and measures its persistency time on the chamber throughout the complete event evolution. A schematic picture of a shower event crossing only two elements of the mosaic is shown in figure 5. The hypothesis is that each detector element triggers the first incoming photon (quantum 1 in the figure) for reference timing so that the read-out of each element works separately. Quantum 1 is read by the drift chamber anodes at time T_1 . Quantum 2 arrives with a delay time Δt which depends upon the energy E of the EECR; it is read at a time T_2 , and so on. The read-out time difference (ΔT) is linked to E , the azimuth (θ) and elevation (Φ) angles of the EECR. Figure 5 indicates with dashed lines a series of pseudo-tracks which are what individual detectors measure. Using the information extracted by all coordinates and interpolating the pseudo-tracks, in principle one derives a sufficient number of constraints to determine the EECR parameters. The second problem is related to the requirement of getting the trigger. A system to extract this information can be obtained with sufficient precision from the chamber itself or from the overhanging MCP.

In a parallel way, another type of projective detector is under development, the Silicon Intensified Micro-Strip detector (SIMS), where a double-sided silicon micro-strip sensor¹⁴ is coupled to the MCP. In this system the strips run orthogonally on the opposite detector surfaces. An ionizing event inside the detector gives origin to a signal on both sides; the crossing point of the particle is derived from the intersection of the two orthogonal projections. The micro-strip system requires a small number of connections and therefore a simple and low power consumption read-out system. The system presents two main problems: the first one is related to the increasing of the noise and of the background which should be integrated along the strips; the second (and more serious) comes from the ambiguity in the coupling of the two coordinates when more than one particle crosses the detector. In low noise and background conditions, this disadvantage can be solved by using the dynamical characteristics of the signal (signal persistency along a straight line).

5. READ-OUT SYSTEM

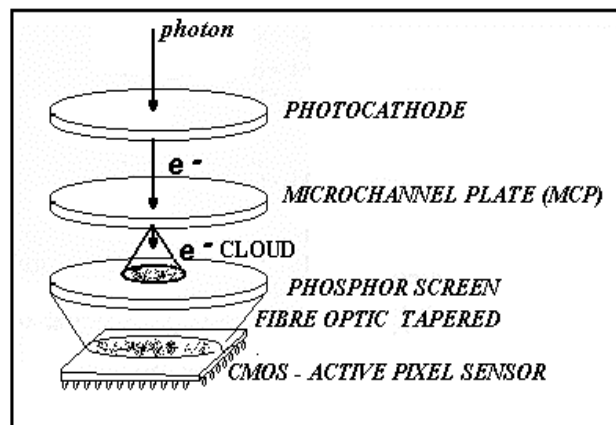
Front End Electronics (FEE) interfacing the surveyed silicon detectors is located close to the detector in order to minimize disturbances and reduce the number of connections. It performs the following main tasks: amplification, shaping and discrimination of the detector signal. The main characteristic of this front end is to reduce the pixel background rate by enhancing the signal to noise ratio: this allows to reduce the processing capability of the on-board computer, in charge of the data analysis, within acceptable limits. In detail, the FEE has to transform the analogue detector signal into a digital pulse for each pixel; it uses a fast single threshold discriminator 1) to count the digitized pulses and enable the output of the pulses after the count has reached a programmable digital threshold, 2) to split the signals for X and Y positions (relevant to the incoming UV photons) and for the timing channel. The pulse count is reset at the end of every integration period (about 1 μ s). To reach the large scale integration necessary to interface the system and process the data, the FEE is realized with ASIC full custom technology. This implementation allows to get the very high speed performances (about 10 ns) with very low power consumption (less than 100 μ W for each pixel) and to minimize the space occupation with respect to the detector sensitive area.

6. CONCLUSIONS

The definition of the best detector for the observation of the nitrogen fluorescence light induced in the atmosphere by very high energy cosmic rays is a very difficult challenge due to the many technical requirements and constraints. At the current stage of investigation, all described systems need to be improved and tested with a strong R&D effort in order to select the detector which better fits the AirWatch requirements.

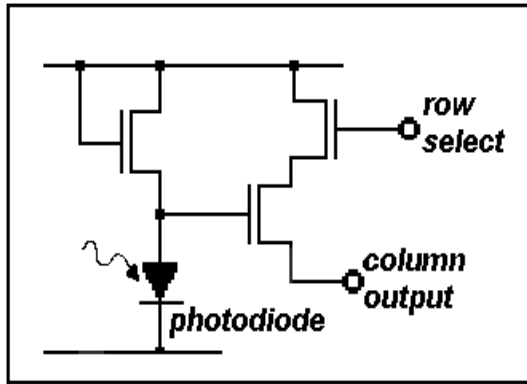
REFERENCES

1. P.Sokolsky: "Introduction to ultrahigh energy cosmic ray physics", 1989, Addison-Wesley; P.Sokolsky, P.Sommers and B.R.Dawson: 1992, Phys. Rep., **217-5**, 225; M.S.Longair : "High energy Astrophysics", 1997, Cambridge University Press.
2. Science, December 1997, **278**, 1708; Physics Today, January 1998, 31; P.L.Biermann: "The origin of the highest energy cosmic rays", 1997, J.Phys. G, **23**, 1.
3. M.Boratav : "The Extremely High Energy Cosmic Rays And The Auger Observatory Project", 1996, Nucl.Ph.B- Proceedings Supplements, **48**, 488.
4. L.M.Barbier et al.:1996, Proposal submitted to NASA; J. Ormes et al.:1997, Proc. 25th ICRC, Durban, South Africa, **5**, 273.
5. P.Attinà, C.N.De Marzo, L.Scarsi, R. Stalio: Possible Scenarios for a "Space AirWatch Mission" Devoted to Observations of Atmospheric Fluorescence", 1997, Advance In Space Research, in press.
6. C.De Marzo et al.: Extreme energy Cosmic Rays (EECR) Observation Capabilities of an 'AirWatch from Space' Mission", 1997, to be published in the proceedings TAUP 97, Gran Sasso, Italy.
7. O.Catalano et al.: Proceedings of this Conference
8. E.Alippi, A.Lenti, P.Attinà A.Gregorio, R.Stalio, P.Trampus, L.Bosisio, G.Giannini, A.Vacchi, V.Gracco, A.Petrolini, G.Piana, O.Catalano, S.Giarrusso, G.Bonanno:"AirWatch: the Fast Detector", 1998, AIP Proceedings, in press.
9. Werner Ogiers: Survey of CMOS Imagers, IMEC, Division MAP, 1997.
10. MAPMT, 1996, Hamamatsu, Electron Tube Products, Condensed Catalog
11. G.Anzivino et al.; 1995, Nucl. Instr. and Meth. In Phys. Res. A, **365**, 76; R.De Salvo et al.; 1997, Nucl. Instr. and Meth. In Phys. Res. A, **387**, 92; E.Chesi et al.: 1997, Nucl. Instr. and Meth. In Phys. Res. A, **387**, 122.
12. G.Bernacchia, V.Bonvicini, A.Monfardini, A.Rashevsky, R.Stalio, A.Vacchi: "Conceptual Development of a New UV Detector: SD 2000", 1997, Opt. Eng., **36**, 2497.
13. S.Beolè et al.: "Steps towards the use of silicon drift detectors in heavy ion collisions at LHC", 1995, Nucl. Instr. and Meth. A, **360**, 67; S.Beolè et al.: "Silicon Drift Detectors; studies about geometry of electrodes and production technology", 1996, Nucl. Instr. and Meth. A, **377**, 393; S.Beolè et al.: "New developments on silicon drift detectors", 1996, Nuovo Cimento, **109A**, 1261.
14. G.Batignani, L.Bosisio, M.Carpinelli, C.Diaconu, P.Elmer, F.Forti, M.Giorgi, G.Rizzo, G.Triggiani: "Results on double-sided d.c.-coupled silicon strip detectors irradiated with photons up to 1 Mrad", 1996, Nuovo Cimento, **109A**, 1309; G.Batignani, L.Bosisio, R.DellaMarina, P.Elmer, F.Forti, M.Giorgi, G.Rampino, G.Rizzo, S.Tritto: "Results on double-sided a.c.-coupled silicon strip detectors", 1996, Nuovo Cimento, **109A**, 1319; G.Batignani, F.Forti, M.Giorgi, G.Rampino, S.Tritto, L.Bosisio, R.DellaMarina: "Characterization of MOS transistors integrated on high resistivity silicon with a DSSD process", 1997, Nuovo Cimento, **110A**, 817.

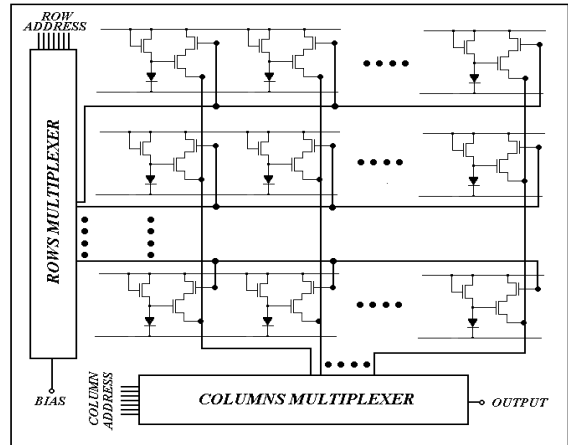


Schematic of the Intensified CMOS-APS (LAPS)

Figure 1

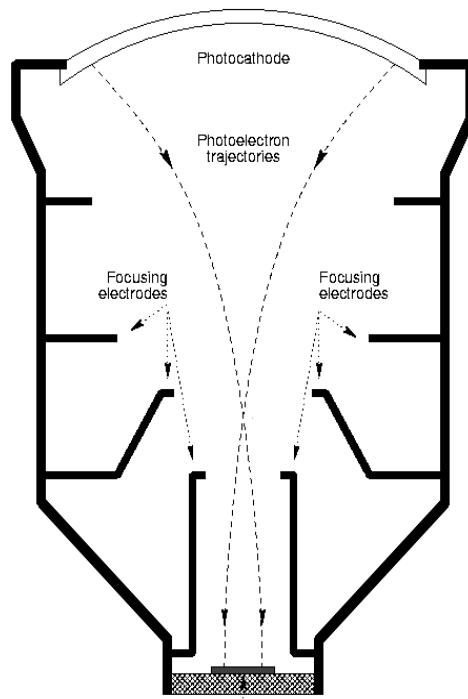


Three Transistor CMOS-Active Pixel



Schematic diagram of a complete CMOS-APS pixel matrix

Figure 2: Three Transistor CMOS-Active Pixel (left) and schematic diagram of a complete CMOS-APS pixel matrix (right).



Silicon detector and Front-end electronics

Figure 3: The HPDT detector.

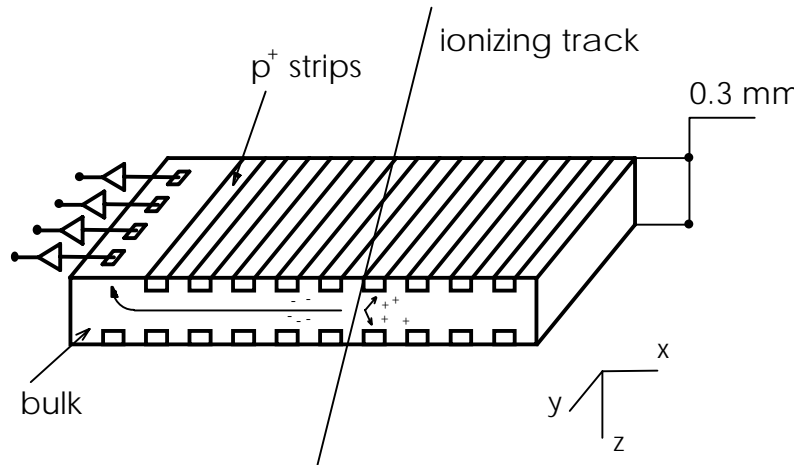


Figure 4: The silicon drift chamber (schematics)

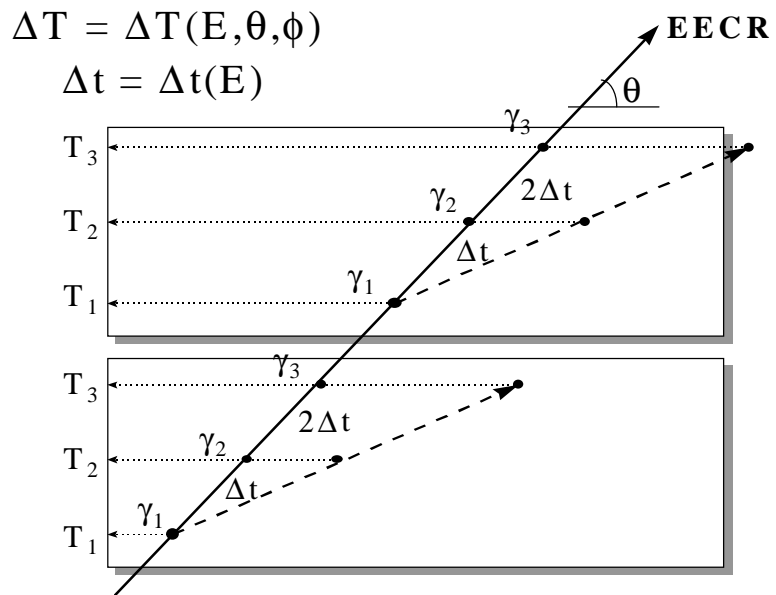


Figure 5: A schematic diagram of an event arriving on a mosaic of drift chamber detectors.